Iğdır Üniversitesi Fen Bilimleri Enstitüsü Dergisi, 15(4), 1343-1353, 2025 Journal of the Institute of Science and Technology, 15(4), 1343-1353, 2025

ISSN: 2146-0574, eISSN: 2536-4618

Physics DOI: 10.21597/jist.1779594

Research Article

Received: 07.09.2025 Accepted: 23.10.2025

To Cite: Bulgurcuoğlu, A. E. (2025). Deposition Sequence Effects in Bilayer Electrodes: Preparation of PANI/ ZnO and ZnO / PANI Via Electrochemical Deposition. *Journal of the Institute of Science and Technology*, 15(4), 1343-1353.

Deposition Sequence Effects in Bilayer Electrodes: Preparation of PANI / ZnO and ZnO / PANI Via Electrochemical Deposition

Ayşe Evrim BULGURCUOĞLU¹

Highlights:

- Deposition sequence strongly affected electrochemical performance.
- PANI/ZnO exhibited superior cycling stability.
- ZnO/PANI showed higher capacitance at high current densities.
- Both bilayers outperformed singlecomponent electrodes

ABSTRACT:

Porous nickel foam was used as a conductive scaffold to fabricate bilayer electrodes composed of polyaniline (PANI) and zinc oxide (ZnO) through electrodeposition. Two sets were prepared: PANI/ZnO, where PANI was deposited first and then coated with ZnO, and ZnO/PANI, where ZnO was deposited first and followed by a PANI layer. Electrochemical characterization demonstrated that the sequence of deposition plays a decisive role in performance. Cyclic voltammetry revealed that PANI/ZnO exhibited broader CV profiles and excellent electrochemical accessibility within the 0-1 V potential window. Galvanostatic charge-discharge tests confirmed that both bilayer electrodes outperformed single-component ZnO and PANI, with ZnO/PANI showing slightly longer discharge times and higher capacitance at increased current densities. Ragone analysis indicated that ZnO/PANI delivered superior energy-power balance under high-rate conditions, whereas PANI/ZnO maintained remarkable cycling stability, retaining nearly its full capacitance after prolonged cycling. These results show that both bilayer configurations benefit from PANI and ZnO, but with distinct advantages: PANI/ZnO is highly stable, while ZnO/PANI is better suited for high-rate applications. The findings highlight the importance of deposition order in optimizing hybrid polymer/oxide.

Keywords:

- PANI/ZnO
- ZnO/PANI
- Electrochemistry
- Supercapacitor
- · Energy storage

^{1*}Ayşe Evrim BULGURCUOĞLU (<u>Orcid ID: 0000-0001-8373-9764</u>), Yıldız Teknik University, Department of Physics, İstanbul, Türkiye

^{*}Corresponding Author: Ayşe Evrim Bulgurcuoğlu, e-mail: bulgurcu@yildiz.edu.tr

INTRODUCTION

The combustion of fossil fuels has led to the depletion of natural reserves while exerting severe negative impacts on ecosystems and accelerating climate change (Qin et al., 2024). To address these challenges, extensive research has focused on the development of greener and more sustainable energy storage systems. Among various alternatives, supercapacitors have emerged as promising devices due to their unique position between conventional capacitors and rechargeable batteries. They combine the high power density and rapid charge—discharge capability of capacitors with the higher energy storage characteristics of batteries, while also offering long cycling life (Lamba et al., 2022; Qin et al., 2024; Wang et al., 2019).

Polyaniline (PANI), a conducting polymer, is widely studied as a pseudocapacitive material (Qin et al., 2024). Owing to its tunable oxidation states, environmental stability, high electrical conductivity, low cost, and facile synthesis, PANI is a suitable candidate for energy storage. Nevertheless, it suffers from several limitations, including agglomeration, reduced effective surface area, and volumetric changes during ion insertion and extraction (doping/dedoping), which result in mechanical degradation (Ahn et al., 2011; Bai et al., 2009; Cheng et al., 2023; Domingues et al., 2011; Rohith et al., 2023). Furthermore, its poor adhesion to current collectors often leads to low specific capacitance (Li et al., 2016). Consequently, both the theoretical capacitance and long-term stability of pristine PANI are negatively affected (Palsaniya et al., 2021).

To overcome these drawbacks, PANI is frequently combined with inorganic or organic nanofillers, or hybridized with metal oxides to improve electrical conductivity and structural stability (Palsaniya et al., 2021). Among various candidates, zinc oxide (ZnO) has attracted considerable attention due to its wide band gap, mechanical strength, chemical stability, nontoxicity, high conductivity, and large exciton binding energy. These characteristics make ZnO highly suitable for energy storage applications (Rahim et al., 2023). Previous studies have demonstrated that ZnO–PANI composites can be successfully applied in different electrochemical systems, where ZnO enhances electrical conductivity, thermal and chemical robustness, and electrode–electrolyte interfacial activity (Foronda et al., 2023; Rahim et al., 2023). Importantly, ZnO also mitigates the volumetric changes of PANI during repeated cycling, thereby improving the overall mechanical durability of the electrode (Liu et al., 2021; Singh et al., 2024; Zhu et al., 2019). ZnO itself has been reported as a high-specific-capacitance electrode material for supercapacitors operating at high current densities (Pradeeswari et al., 2019; Yılmaz et al., 2020). Moreover, combining n-type ZnO with p-type PANI creates a p-n heterojunction structure, which enriches electroactive redox sites and promotes pseudocapacitive behavior (Mahajan et al., 2025)

MATERIALS AND METHODS

Electrode Preparation

Bilayer electrodes composed of polyaniline (PANI) and zinc oxide (ZnO) were fabricated on porous nickel foam via electrochemical deposition using LiClO₄ as the supporting electrolyte. Porous nickel foams (2 × 3 cm) were first cleaned to eliminate surface impurities and native oxides by immersion in 37% HCl, followed by ultrasonic treatment for 3 minutes. The foams were then thoroughly rinsed with deionized water and dried prior to deposition.

Deposition of PANI on Nickel Foam

PANI was deposited in a two-electrode configuration, with nickel foam serving as the working electrode and a platinum sheet $(2 \times 3 \text{ cm})$ as the counter electrode. PANI coating was performed by electrophoretic deposition (EPD) using a stable suspension of pre-synthesized polyaniline powder. A

total of 0.2 g of PANI (emeraldine base form, ≥99% purity, Sigma-Aldrich) was dispersed in 50 mL of 1 M HCl solution and ultrasonicated for 30 min to ensure complete protonation and homogeneous dispersion of PANI–H⁺ chains.

EPD was carried out in a two-electrode setup using nickel foam $(2 \times 3 \text{ cm})$ as the negatively biased electrode and a platinum sheet of equal size as the counter electrode, with a 2 cm inter-electrode gap. A constant voltage of 8 V was applied for 1600 seconds at room temperature. The positively charged PANI–H⁺ particles migrated toward the cathodic Ni foam and formed a uniform nanofibrous film upon drying.

Deposition of ZnO on Nickel Foam

ZnO coating was obtained by electrophoretic deposition (EPD) from a suspension containing presynthesized ZnO nanoparticles (0.5 g /L) in 0.1 M LiClO₄ aqueous solution. The dispersion was sonicated for 20 min prior to deposition. The process was performed at 25 V for 5 min with 2 cm electrode spacing at room temperature.

SEM analysis (Figure 1b) revealed that the ZnO coating exhibited a granular and porous structure, effectively increasing the available electroactive surface area. EDS confirmed the strong Zn contribution (Figure 1c and d). Such morphology promotes ion transport and provides abundant active sites for charge storage. Nevertheless, the inherently low electrical conductivity of ZnO restricts its capacitance performance when used alone, making it more effective in hybrid configurations with conducting polymers such as PANI.

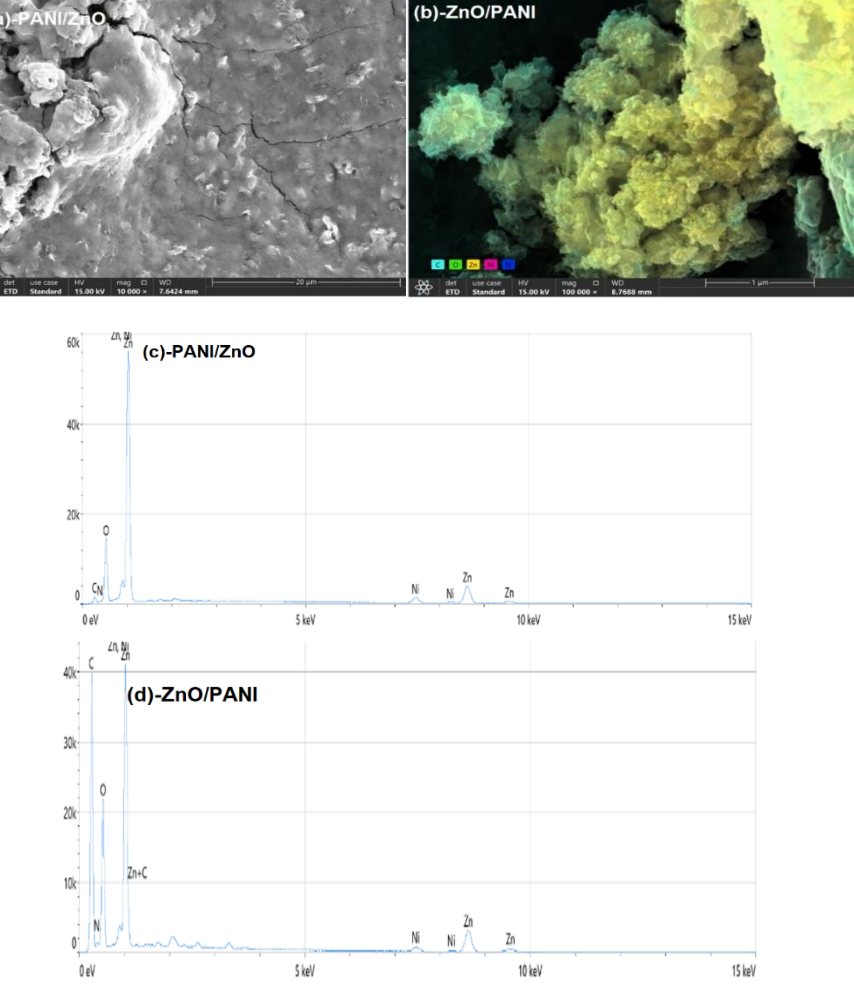


Figure 1. Surface Morphology and Elemental Analysis of PANI/ZnO and ZnO/PANI Bilayer Electrodes

RESULTS AND DISCUSSION

Figure 1 presents the surface morphologies of the bilayer electrodes and their elemental composition obtained by energy-dispersive spectroscopy (EDS). The SEM images of the PANI-coated nickel foam reveal a nanofibrous and irregularly aggregated structure.

Although only surface SEM and EDS datas are presented in this study, the sequential deposition of the bilayers was verified by controlled fabrication steps and complementary surface analysis. Each layer was deposited separately on identical Ni foams to ensure reproducibility and layer isolation. Such morphology is highly beneficial for supercapacitor electrodes as it increases the effective surface area and provides additional pathways for electrolyte ion penetration during charge—discharge processes. In contrast, ZnO deposition produced a granular and porous morphology, which offers a large surface area with abundant electroactive sites. However, due to its inherently low electrical conductivity, ZnO alone cannot provide sufficient charge transfer efficiency.

The bilayer configurations highlight the importance of deposition sequence. In the PANI/ZnO electrode, the conductive PANI layer is buried beneath the outer ZnO coating. While the ZnO surface contributes additional porosity and stability, its poor conductivity partially hinders ion/electron transport, resulting in limited overall capacitive behavior. On the other hand, the ZnO/PANI electrode exhibits better structrure: the ZnO underlayer provides a mechanically stable and porous scaffold, while the outer PANI layer establishes a conductive interface directly exposed to the electrolyte. This configuration ensures enhanced redox activity and facilitates faster charge transfer.

EDS analysis confirms the elemental composition of both bilayers. Strong Zn and O signals dominate the PANI/ZnO sample, consistent with the ZnO-rich surface. In contrast, the ZnO/PANI electrode shows higher intensities of C and N peaks, which correspond to the outer PANI coating. This elemental distribution validates that the topmost layer dictates the dominant surface chemistry of the bilayer electrodes.

Overall, the SEM and EDS analyses demonstrate that the ZnO/PANI bilayer provides a more required morphology for efficient ion transport and electrochemical activity, which is expected to translate into superior specific capacitance and cycling stability compared to the PANI/ZnO configuration.

The cyclic voltammetry (CV) curves of the bilayer electrodes (Figure 2) reveal the strong influence of deposition sequence on capacitive performance. All electrochemical characterizations (cyclic voltammetry, galvanostatic charge–discharge, and impedance measurements) were performed using a Gamry Interface 1010E potentiostat in a two-electrode configuration. Both electrodes consisted of 2×3 cm Ni foam pieces, one coated with the active material and the other serving as the counter electrode. The electrolyte was 0.2 M Na₂SO₄ aqueous solution, which is electrochemically stable within the applied potential window of 0–1 V. All measurements were carried out at room temperature.

The CV tests were conducted at scan rates of 20, 50, 100, 150, and 200 mV/s, while the GCD measurements were performed at discharge currents between 1mA and 5mA. For consistency, all capacitance and current values are reported as specific current densities (A/g), normalized to the active mass of a single electrode (2.5 mg). No IR-drop correction was applied, as the internal resistance remained low and comparable across all samples.

In our measurements, the PANI/ZnO electrode exhibited a broader CV area compared to the ZnO/PANI electrode over the 0–1 V potential window. This indicates that, under the present experimental conditions, PANI/ZnO delivered higher charge storage capacity. The redox peaks observed

in both electrodes originate from the reversible dopping-dedopping processes of PANI, confirming its pseudocapacitive contribution.

The narrower CV area of ZnO/PANI can be explained by two factors. First, ZnO served as the underlayer, and its fractured, glass-like morphology may have limited effective ion transport pathways. Second, the relatively narrow 0–1 V window restricted the activation of PANI's higher-potential redox transitions when PANI was positioned as the outer layer. As a result, part of the pseudocapacitive contribution of the PANI coating was clipped within this voltage range, leading to an underestimation of the ZnO/PANI electrode's performance.

At low scan rates, both electrodes showed clear redox features, but as the scan rate increased, the difference between the two configurations became more pronounced: PANI/ZnO retained a larger enclosed area, while ZnO/PANI experienced stronger suppression of its electrochemical response. A direct comparison at 150 mV /s highlights this trend, where the CV profile of PANI/ZnO is visibly broader than that of ZnO/PANI. For reference, the individual curves of bare PANI and ZnO electrodes confirm that PANI inherently contributes much higher capacitance than ZnO, underscoring the importance of preserving its accessibility in bilayer structures.

Figure 3 compares the galvanostatic charge–discharge (GCD) behaviors of bare ZnO, bare PANI, and the two bilayer electrodes at a constant current of 1 mA. All electrodes display nearly triangular and symmetric charge–discharge curves, which indicates good capacitive reversibility and high Coulombic efficiency. However, the discharge times and curve shapes reveal clear differences in their electrochemical performances.

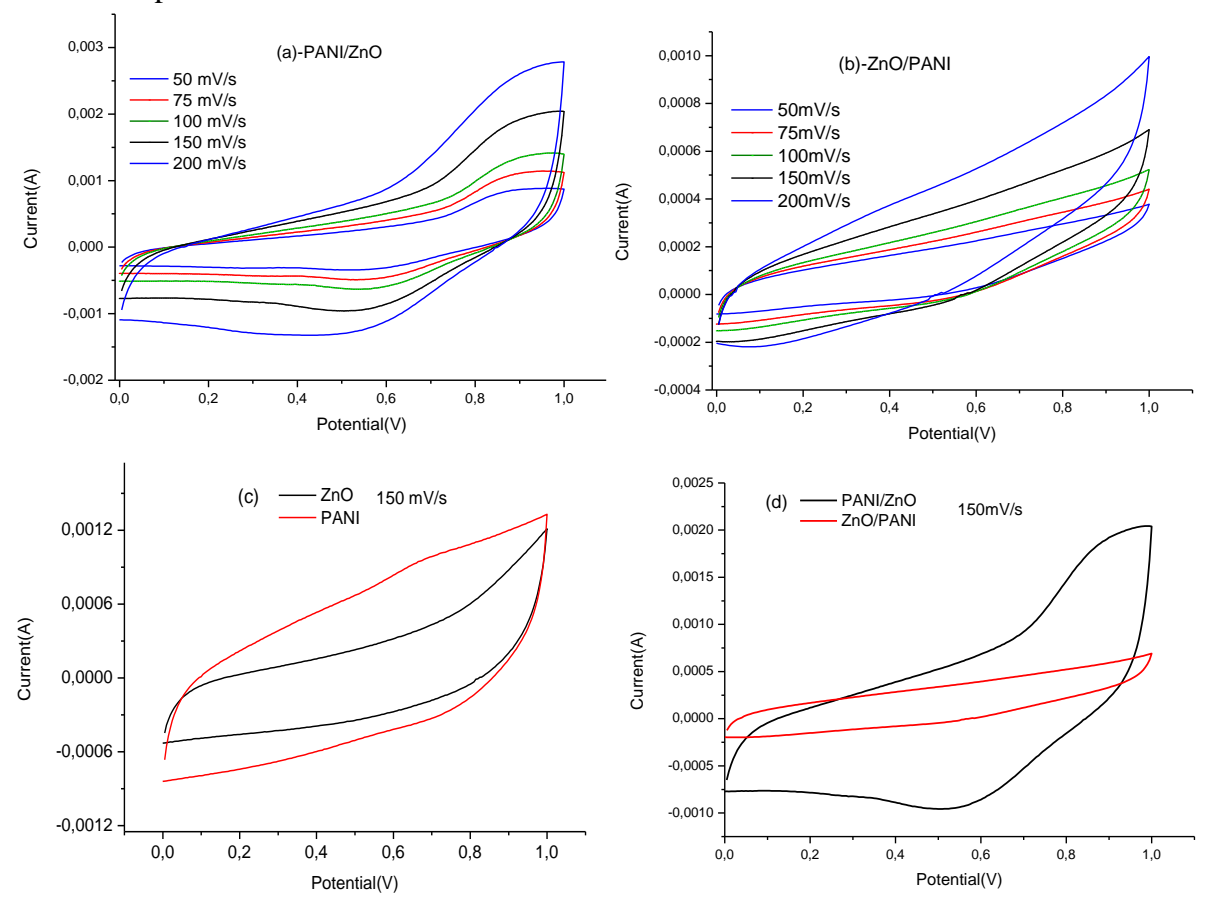


Figure 2. Cyclic Voltammetry Behavior of PANI/ZnO (a) and ZnO/PANI (b) Electrodes at Different Scan Rates (c) ZnO and PANI at 150 mV/s (d) PANI/ZnO and ZnO/PANI electrodes at 150 mV/s

For the ZnO electrode (Figure 3a), the discharge curves are relatively short, reflecting the limited capacitance of ZnO. Although ZnO provides a porous structure and mechanical stability, its intrinsically low electrical conductivity restricts its ability to store large amounts of charge.

For the PANI electrode (Figure 3b), the discharge times are considerably longer compared to ZnO. This result is consistent with the pseudocapacitive nature of PANI, which relies on fast and reversible redox reactions to deliver higher capacitance. Nevertheless, the slight distortion of the triangular shape also indicates the presence of internal resistance and the tendency of PANI to undergo structural changes during charge—discharge cycling.

The bilayer electrodes (Figure 3c) demonstrate how the deposition sequence directly impacts capacitive behavior. Both PANI/ZnO (blue curve) and ZnO/PANI (red curve) show much longer discharge times than the individual components, confirming the beneficial effect of combining the two materials. Interestingly, in this measurement, the ZnO/PANI electrode exhibits a slightly longer discharge time than PANI/ZnO, suggesting a marginally higher specific capacitance. This observation contrasts with the CV analysis, where PANI/ZnO showed a larger enclosed area in the 0–1 V window. The difference highlights the fact that capacitance evaluation is highly dependent on the testing method and voltage range.

The slightly better GCD performance of ZnO/PANI can be explained by the synergistic effect of the bilayer structure. The ZnO underlayer provides a porous and mechanically robust foundation, while the outer PANI layer ensures rapid electron transfer and electroactive redox reactions. Even though the CV results suggested suppressed activity for ZnO/PANI under the chosen potential window, the galvanostatic test demonstrates that the electrode can effectively utilize its active sites during charge—discharge at constant current.

In summary, Figure 3 shows that both bilayer configurations outperform the individual components, confirming the synergistic advantage of combining PANI and ZnO. Moreover, the slight difference in discharge times between PANI/ZnO and ZnO/PANI emphasizes that deposition order influences performance, but the results may vary depending on the electrochemical testing method.

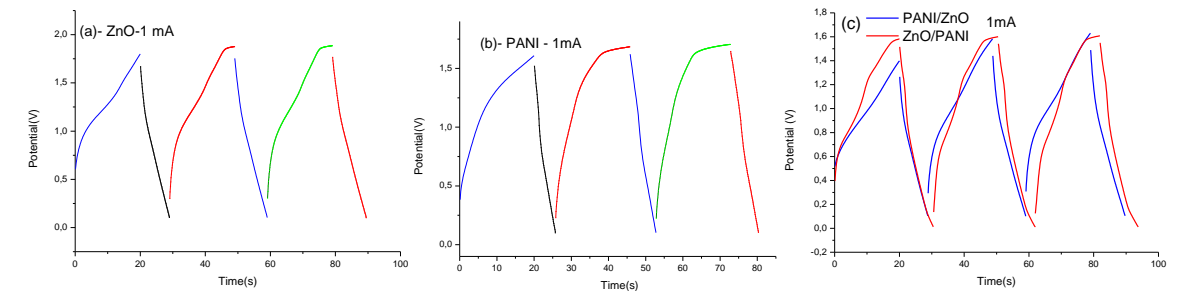


Figure 3. Galvanostatic Charge–Discharge Profiles of ZnO (a), PANI (b), and bilayer electrodes (c) at 1 mA

The variation of specific capacitance with applied current reveals important insights into the rate capability of the bilayer electrodes in Figure 4(a).

The specific capacitance (C, F/g) was determined from the discharge segment of the GCD profiles according to Eq. (1) (Yargi et al., 2020):

$$C = I\Delta t/m\Delta V \tag{1}$$

Here, I denotes the applied discharge current (A), Δt represents the discharge time (s), m corresponds to the mass of the active electrode material (g), and ΔV is the potential window during the discharge process (V).

At low currents (1–2 mA), both PANI/ZnO and ZnO/PANI exhibit comparable capacitance values, indicating that both configurations can efficiently utilize their active materials when the charge—discharge process is relatively slow. However, as the current increases, the difference between the two structures becomes more evident. The ZnO/PANI electrode shows a sharper rise in capacitance at higher currents (up to 5 mA), surpassing PANI/ZnO. This trend suggests that ZnO/PANI benefits from the synergistic contribution of the porous ZnO scaffold and the conductive outer PANI layer, which together allow for more efficient ion transport and electron conduction at elevated charge—discharge rates. In contrast, the PANI/ZnO electrode, with ZnO as the outer layer, faces increased resistance and reduced accessibility of its electroactive sites, leading to relatively lower capacitance growth at high currents. The Ragone plot further clarifies the performance differences between the two bilayer electrodes.

The energy density (E, Wh/kg) and power density (P, W/kg) of the prepared electrodes were obtained using the following expressions (Yargi et al., 2020):

$$E = \frac{1}{72} \text{CV}^2 \times 3600 \tag{2}$$

$$P = E/t \tag{3}$$

In these formulas, C is the calculated specific capacitance in farads per gram, ΔV indicates the discharge potential window in volts, and Δt corresponds to the discharge time in seconds.

Both configurations follow the typical trend of decreasing energy density as power density increases, reflecting the trade-off between high charge storage and rapid charge delivery. However, the ZnO/PANI electrode consistently maintains higher energy densities across the full range of power outputs. At moderate power levels, ZnO/PANI reaches an energy density peak exceeding that of PANI/ZnO, while at higher power densities it sustains a larger fraction of its initial energy density. Both electrodes show the expected Ragone trend of decreasing energy density with increasing power density. At lower power densities (1–2 kW k/g), PANI/ZnO achieves energy densities of 25–30 Wh k/g, while ZnO/PANI is slightly lower at 20–25 Wh k/g. However, as power density rises to the range of 10–50 kW k/g, ZnO/PANI begins to outperform PANI/ZnO, sustaining energy densities around 100–110 Wh k/g, compared to PANI/ZnO's 95–100 Wh k/g

This performance highlights the structural advantage of ZnO/PANI: the porous ZnO underlayer provides robust ion diffusion channels, while the outer PANI layer contributes fast redox activity and electrical conductivity.

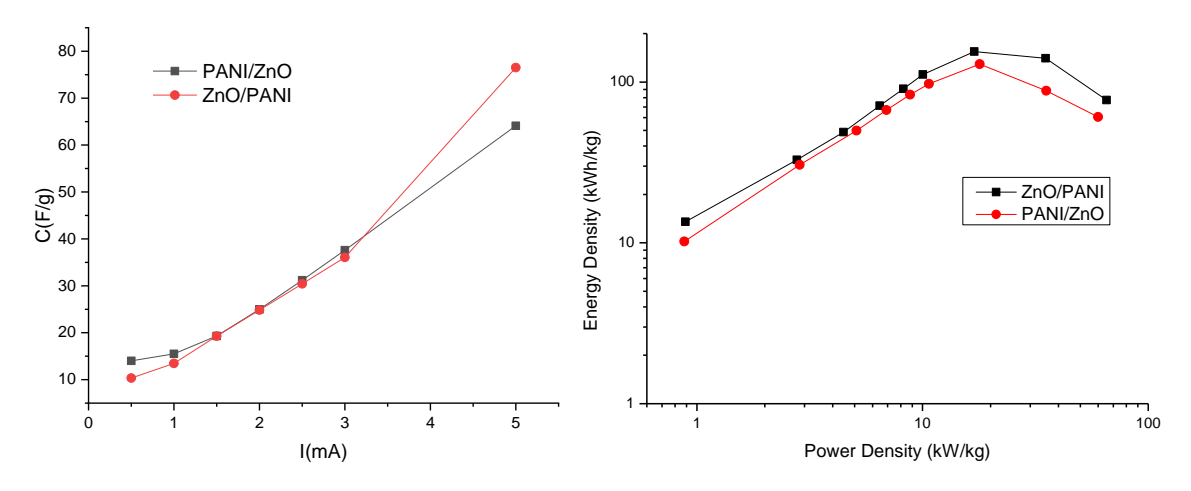


Figure 4. Specific Capacitances of Bilayer Electrodes and Energy Density vs. Power Density of PANI/ZnO and ZnO/PANI

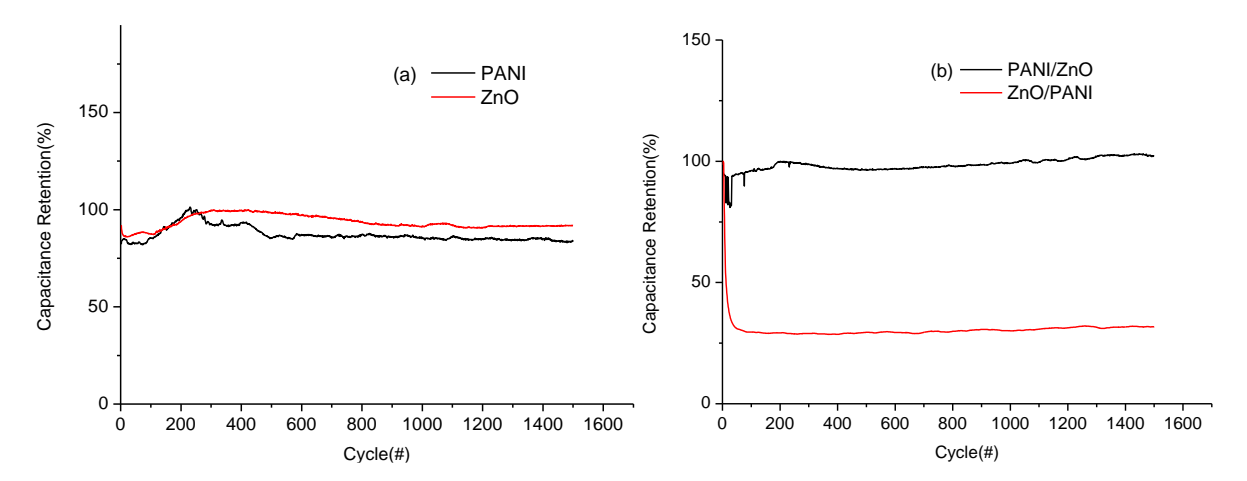


Figure 5. Capacitance Retention of (a) PANI, ZnO and (b) Bilayer Electrodes

The cycling performance of pure PANI and pure ZnO electrodes was tested up to 1500 cycles in Fig 5. Both electrodes retained a significant fraction of their initial capacitance, but clear differences are observed. PANI showed a gradual decrease, stabilizing around 85–90% retention after 1500 cycles. ZnO, on the other hand, retained slightly higher values, close to 90–95% retention at the end of the test. These results confirm that while PANI offers high capacitance, its mechanical swelling and structural degradation during repeated dopping/dedopping lead to moderate fading. ZnO, though less capacitive, contributes better structural stability. The seemingly contradictory behavior of the ZnO/PANI electrode excellent rate performance but poor long-term cycling stability arises from its structural characteristics.

The ZnO underlayer exhibits a cracked, glass-like morphology (as shown in Figure 6) that provides open ion channels and facilitates fast ion/electron transport at high charge—discharge rates. This explains the high specific capacitance and superior energy—power performance observed at elevated currentdensities.

However, the same fragile ZnO structure weakens the mechanical integrity of the bilayer during repeated cycling, leading to partial delamination of the outer PANI coating and loss of electrical contact. This results in the early capacity drop within the first 100 cycles, after which the electrode stabilizes. A striking difference is observed between PANI/ZnO and ZnO/PANI. The PANI/ZnO electrode (black curve) demonstrates excellent stability: after an initial slight fluctuation, it stabilizes and even shows a small upward trend, maintaining nearly 100–105% of its initial capacitance after 1500 cycles. This suggests that the buried PANI layer remains electrochemically accessible, while the ZnO top layer provides mechanical robustness that prevents severe degradation.

In contrast, the ZnO/PANI electrode (red curve) suffers from a sharp capacitance drop in the very early cycles, losing almost 60–70% of its initial value within the first 100 cycles. After this sudden decrease, the capacitance stabilizes but remains at only about 30–35% of the initial capacitance throughout the rest of the cycling test. This behavior can be explained by the fragile ZnO underlayer morphology observed in Figure 6, which exhibits cracked, glass-like structures. Such a structure may fail to support the outer PANI coating during repeated charge–discharge, leading to poor adhesion, loss of active material, and limited ion/electron transport pathways.

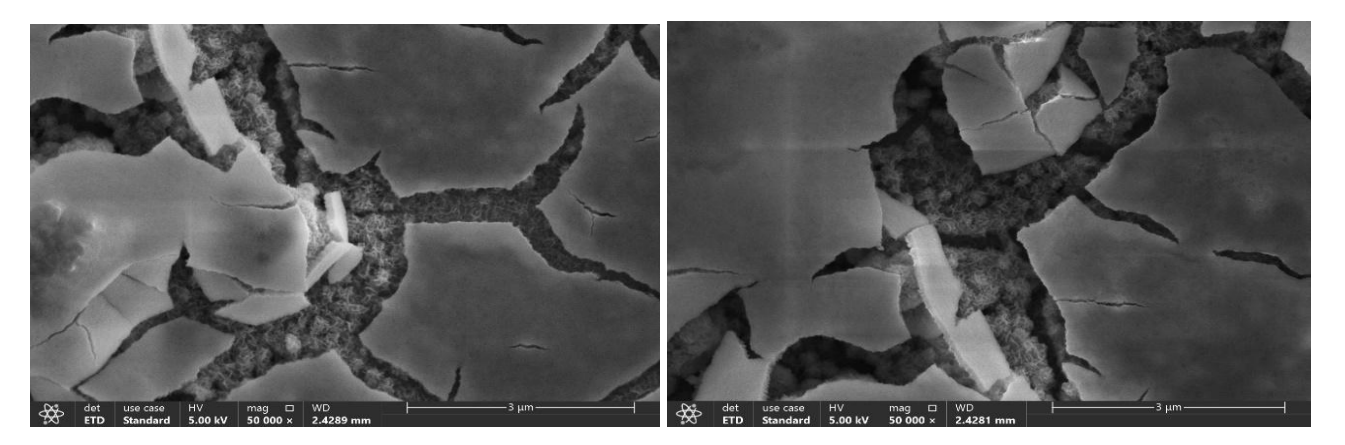


Figure 6. SEM images of ZnO/PANI Electrode

CONCLUSION

In this work, bilayer electrodes composed of polyaniline (PANI) and zinc oxide (ZnO) were successfully fabricated on porous nickel foam by electrodeposition. Two different set were prepared: PANI/ZnO, where PANI was deposited first and then coated with ZnO, and ZnO/PANI, where ZnO was deposited first and followed by a PANI layer.

Electrochemical analyses revealed that the performance of the electrodes strongly depends on the deposition sequence. CV and GCD measurements demonstrated that both bilayer electrodes outperformed the single-component ZnO and PANI electrodes, confirming the beneficial effect of combining a conductive polymer with a porous oxide. However, differences emerged between the two configurations. PANI/ZnO exhibited broader CV areas and excellent long-term cycling stability, maintaining nearly full capacitance after extended cycling. On the other hand, ZnO/PANI displayed slightly longer discharge times and higher capacitance at higher current densities, as well as superior energy—power balance in the Ragone plot, confirming its advantage for high-rate applications.

These results highlight that the deposition sequence plays a decisive role in determining electrochemical behavior. While PANI/ZnO offers remarkable durability, ZnO/PANI provides better high-rate capability. Together, these findings suggest that rational control over layer ordering enables the optimization of hybrid polymer/oxide electrodes. Such bilayer structures are therefore promising candidates for the development of high-performance and application-specific supercapacitors.

ACKNOWLEDGEMENTS

This work was supported by Yıldız Technical University Scientific Research Projects Coordinator's project numbered FBA-2021-4279.

Conflict of Interest

There is no conflict of interest.

Author's Contributions

The author has completed all stages of the study.

REFERENCES

Ahn, D., Yoo, I., Koo, Y. M., Shin, N., Kim, J., & Shin, T. J. (2011). Effects of cobalt-intercalation and polyaniline coating on electrochemical performance of layered manganese oxides. *Journal of Materials Chemistry*, 21(14), 5282–5289. https://doi.org/10.1039/c0jm03548c

- Bai, H., Xu, Y., Zhao, L., Li, C., & Shi, G. (2009). Non-covalent functionalization of graphene sheets by sulfonated polyaniline. *Chemical Communications*, *13*, 1667–1669. https://doi.org/10.1039/b821805f
- Cheng, T. M., Yen, S. C., Hsu, C. S., Wang, W. T., Yougbaré, S., Lin, L. Y., & Wu, Y. F. (2023). Novel synthesis of polyaniline, manganese oxide and nickel sulfide lavandula-like composites as efficient active material of supercapacitor. *Journal of Energy Storage*, 66. https://doi.org/10.1016/j.est.2023.107390
- Domingues, S. H., Salvatierra, R. V., Constantinides, C. P., Zarbin, A. J. G., Eisler, D. J., & Rawson, J. M. (2011). Transparent and conductive thin films of graphene/polyaniline nanocomposites prepared through interfacial polymerization. *Chemical Communications*, 47(9), 2592–2594. https://doi.org/10.1039/c0cc04304d
- Foronda, J. R. F., Aryaswara, L. G., Santos, G. N. C., Raghu, S. N. V., & Muflikhun, M. A. (2023). Broad-class volatile organic compounds (VOCs) detection via polyaniline/zinc oxide (PANI/ZnO) composite materials as gas sensor application. *Heliyon*, *9*(2). https://doi.org/10.1016/j.heliyon.2023.e13544
- Kalambate, P. K., Rawool, C. R., Karna, S. P., & Srivastava, A. K. (2019). Nitrogen-doped graphene/palladium nanoparticles/porous polyaniline ternary composite as an efficient electrode material for high performance supercapacitor. *Materials Science for Energy Technologies*, 2(2), 246–257. https://doi.org/10.1016/j.mset.2018.12.005
- Lamba, P., Singh, P., Singh, P., Singh, P., Bharti, Kumar, A., Gupta, M., & Kumar, Y. (2022). Recent advancements in supercapacitors based on different electrode materials: Classifications, synthesis methods and comparative performance. In *Journal of Energy Storage* (Vol. 48). Elsevier Ltd. https://doi.org/10.1016/j.est.2021.103871
- Liu, Y., Dai, Z., Zhang, W., Jiang, Y., Peng, J., Wu, D., Chen, B., Wei, W., Chen, X., Liu, Z., Wang, Z., Han, F., Ding, D., Wang, L., Li, L., Yang, Y., & Huang, Y. (2021). Sulfonic-Group-Grafted Ti3C2TxMXene: A Silver Bullet to Settle the Instability of Polyaniline toward High-Performance Zn-Ion Batteries. *ACS Nano*, *15*(5), 9065–9075. https://doi.org/10.1021/acsnano.1c02215
- Li, X., Zhang, C., Xin, S., Yang, Z., Li, Y., Zhang, D., & Yao, P. (2016). Facile Synthesis of MoS2/Reduced Graphene Oxide@Polyaniline for High-Performance Supercapacitors. *ACS Applied Materials and Interfaces*, 8(33), 21373–21380. https://doi.org/10.1021/acsami.6b06762
- Mahajan, P., Sardana, S., & Mahajan, A. (2025). Ternary MXene/PANI/ZnO-based composite with a built-in p-n heterojunction for high-performance supercapacitor applications. *Journal of Physics D: Applied Physics*, *58*(4). https://doi.org/10.1088/1361-6463/ad875a
- Palsaniya, S., Nemade, H. B., & Dasmahapatra, A. K. (2021). Hierarchical PANI-RGO-ZnO ternary nanocomposites for symmetric tandem supercapacitor. *Journal of Physics and Chemistry of Solids*, 154. https://doi.org/10.1016/j.jpcs.2021.110081
- Pradeeswari, K., Venkatesan, A., Pandi, P., Karthik, K., Hari Krishna, K. V., & Mohan Kumar, R. (2019). Study on the electrochemical performance of ZnO nanoparticles synthesized via non-aqueous sol-gel route for supercapacitor applications. *Materials Research Express*, 6(10). https://doi.org/10.1088/2053-1591/ab3cae
- Qin, D., Zhou, B., Li, Z., & Yang, C. (2024). Construction of controllable multicomponent ZnO-ZnCo/MOF-PANI composites for supercapacitor applications. *Journal of Molecular Structure*, *1309*. https://doi.org/10.1016/j.molstruc.2024.138140

- Rahim, M., Yaseen, S., & Ullah, R. (2023). Electrochemical supercapacitor based on polyaniline/bismuth-doped zinc oxide (PANI/Bi–ZnO) composite for efficient energy storage. *Journal of Physics and Chemistry of Solids*, *182*. https://doi.org/10.1016/j.jpcs.2023.111610
- Rohith, R., Thejas Prasannakumar, A., Manju, V., R. Mohan, R., & J. Varma, S. (2023). Flexible, symmetric supercapacitor using self-stabilized dispersion-polymerised polyaniline/V2O5 hybrid electrodes. *Chemical Engineering Journal*, 467. https://doi.org/10.1016/j.cej.2023.143499
- Singh, R., Agrohiya, S., Rawal, I., Ohlan, A., Dahiya, S., Punia, R., & Maan, A. S. (2024). Multifunctional porous polyaniline/phosphorus-nitrogen co-doped graphene nanocomposite for efficient room temperature ammonia sensing and high-performance supercapacitor applications. *Applied Surface Science*, 665. https://doi.org/10.1016/j.apsusc.2024.160368
- Wang, Y., Liu, Y., Wang, H., Liu, W., Li, Y., Zhang, J., Hou, H., & Yang, J. (2019). Ultrathin NiCo-MOF Nanosheets for High-Performance Supercapacitor Electrodes. *ACS Applied Energy Materials*, 2(3), 2063–2071. https://doi.org/10.1021/acsaem.8b02128
- Yılmaz, İ., Gelir, A., Yargi, O., Sahinturk, U., & Ozdemir, O. K. (2020). Electrodeposition of zinc and reduced graphene oxide on porous nickel electrodes for high performance supercapacitors. *Journal of Physics and Chemistry of Solids*, 138. https://doi.org/10.1016/j.jpcs.2019.109307
- Zhu, C., He, Y., Liu, Y., Kazantseva, N., Saha, P., & Cheng, Q. (2019). ZnO@MOF@PANI core-shell nanoarrays on carbon cloth for high-performance supercapacitor electrodes. *Journal of Energy Chemistry*, *35*, 124–131. https://doi.org/10.1016/j.jechem.2018.11.006